CHEMISTRY
A EUROPEAN JOURNAL

DOI: 10.1002/chem.200600413

Light-Harvesting Metallosupramolecular Squares Composed of Perylene Bisimide Walls and Fluorescent Antenna Dyes

Chang-Cheng You, Catharina Hippius, Matthias Grüne, and Frank Würthner*[a]

Dedicated to Dr. Volker Böhmer on the occasion of his 65th birthday

Abstract: The fluorescent dye 4-dimethylamino-1,8-naphthalimide was incorporated at the bay area of *N*,*N*′-bispyridyl perylene bisimide to afford a fourfold-functionalized perylene bisimide ligand. Through self-assembly directed by metal-ion coordination, a multichromophore supramolecular entity composed of sixteen dimethylaminonaphthalimide antennas and a perylene bisimide-walled square core was subsequently constructed from this linear ditopic ligand and 90° metal corner [Pd(dppp)](OTf)$_2$ (dppp = 1,3-bis(diphenylphosphino)propane; OTf = trifluoromethanesulfonate) in good yield. The isolated metallosupramolecular square was characterized by elemental analysis and ^{1}H, ^{13}C, and ^{31}P{^{1}H} NMR and UV/Vis spectroscopy. Furthermore, by means of ^{1}H NMR diffusion-ordered spectroscopy (DOSY) the dimension of this assembly was evaluated by employing a previously reported perylene bisimide ligand and its square assembly as references. The results obtained confirm the square framework of the current assembly. The optical properties of this multichromophore dye assembly were investigated by UV/Vis and steady-state and time-resolved fluorescence spectroscopy. It was revealed that light captured by dimethylaminonaphthalimide antennas could be efficiently transported to the perylene bisimide core by a fluorescence resonance mechanism (energy-transfer efficiency $E = 95\,\%$), and this resulted in almost exclusive detection of intense perylene bisimide emission, irrespective of the excitation wavelength applied. The present square scaffold containing aminonaphthalimide antenna dyes exhibits more than seven times higher fluorescence quantum yield ($\Phi_{fl} = 0.37$) than a previously reported pyrene-bearing perylene bisimide-walled square ($\Phi_{fl} = 0.05$). Thus, this multichromophore square assembly with aminonaphthalimide antenna dyes is an artificial model for the cyclic light-harvesting complexes in purple bacteria.

Keywords: dyes/pigments · palladium · photochemistry · self-assembly · supramolecular chemistry

Introduction

Photosynthesis in higher plants and numerous bacteria is one of the most important processes in biological systems. It has been demonstrated that the primary steps of photosynthesis in purple bacteria involve absorption of photons by light-harvesting (LH) complexes and subsequent transport of the energy through excited-state energy transfer to the photosynthetic reaction centers.[1] Structural analysis revealed that in the LH1 and LH2 complexes of purple bacteria, bacteriochlorophyll dyes are noncovalently bound to proteins in a circular or elliptical topology, and the cyclic arrays act as the fundamental structural feature for their functionality.[2] In the past, enormous efforts have been devoted to understanding the highly efficient light-harvesting capabilities of LH complexes. On the one hand, artificial multichromophore counterparts have been developed,[3] and especially dendritic dye assemblies became popular during the past few years for mimicking the functionality of light harvesting and energy transfer.[4] On the other hand, supramolecular methodology has also been utilized to construct macrocyclic dye assemblies from the viewpoint of structural resemblance.[5] Cyclic dye assemblies are superior to architectures of other topologies in the following respects: First, circular structures are suited for generating densely packed two-dimensional arrays that facilitate further hierarchical self-assembly processes on appropriate surface materials. Second, macrocyclic assemblies have inherent cavities for the encapsulation of guest molecules and may potentially

[a] Dr. C.-C. You, C. Hippius, Dr. M. Grüne, Prof. F. Würthner
Institut für Organische Chemie
Universität Würzburg
Am Hubland, 97074 Würzburg (Germany)
Fax: (+49) 931-888-4756
E-mail: wuerthner@chemie.uni-wuerzburg.de

serve as a photochemical reactor by harnessing the energy captured by peripheral dye molecules. Nevertheless, supramolecular assemblies bearing both structural and functional features of LH complexes in purple bacteria have been rarely reported so far.

Over the past decade, self-assembly directed by metal coordination has proven to be one of the most powerful tools to construct discrete supramolecular macrocycles through thermodynamic control.[5,6] By utilizing this approach, we have previously prepared a number of supramolecular squares based on perylene bisimide dyes, which show interesting optical and electrochemical properties.[7] As natural light-harvesting systems are comprised of different types of dyes and contain larger numbers of dye units than reported monochromophore square assemblies, we incorporated additional chromophoric units such as pyrenes to obtain multichromophore square scaffold **2a** with four perylene bisimide units as core and sixteen pyrene units as antenna chromophores (Scheme 1).[8] However, recent in-depth photophysical investigations revealed that in metallosupramolecular square **2a**, besides fast energy transfer, ultrafast and highly efficient electron transfer from the pyrene antenna chromophores to the central perylene bisimide dyes strongly quenches the fluorescence emission of perylene bisimide.[9] To develop more efficient light-harvesting systems based on multichromophore square scaffolds that are structurally and functionally reminiscent of natural LH complexes (e.g., in purple bacteria), we searched for alternative antenna chromophores which are capable of efficient photoinduced energy transfer but do not diminish the fluorescence emission of perylene bisimide.

High fluorescence quantum yields of the chromophores and a proper spectral overlap between the fluorescence emission band of the energy-donor dye and the absorption band of the energy-acceptor dye are two crucial prerequisites for the design of dye arrays with efficient Förster-type fluorescence resonance energy transfer (FRET) properties. Furthermore, separated absorption bands of the dye components are advantageous, as they can be excited individually. Under consideration of the above-mentioned aspects, 4-amino-1,8-naphthalimide derivatives appear to be promising antenna dyes for light-harvesting multichromophore square arrays based on perylene bisimides, since they exhibit absorption maxima around 400 nm and emit a strong green fluorescence ($\lambda_{em} \approx 500$ nm, $\Phi_{fl} \approx 0.8$) in less polar solvents such as hexane and dioxane.[10] In this context, such aminonaphthalimide dyes may serve as the light-input molecules that transport the absorbed energy to perylene bisimide through a FRET mechanism. Therefore, we have designed a new ditopic perylene bisimide ligand **1b** (Scheme 1) which contains highly fluorescent 4-dimethylamino-1,8-naphthalimide dyes at the bay area of perylene bisimide. As the fluorescence emission of dimethylaminonaphthalimide substantially overlaps with the absorption bands of the perylene bisimide dye, FRET is envisioned to be efficient in multichromophore systems that are composed of these two dyes. Here we report that metal-ion-directed supramolecular self-assembly of the newly designed perylene bisimide building block **1b** leads to square array **2b**, which incorporates four inner perylene bisimide dyes and sixteen aminonaphthalimide antenna dyes. The optical and photophysical properties of aminonaphthalimide-functionalized perylene bisimide ligand **1b** and square **2b** were investigated in detail and compared with those of the previously reported pyrene-functionalized systems **1a** and **2a**.[8,9]

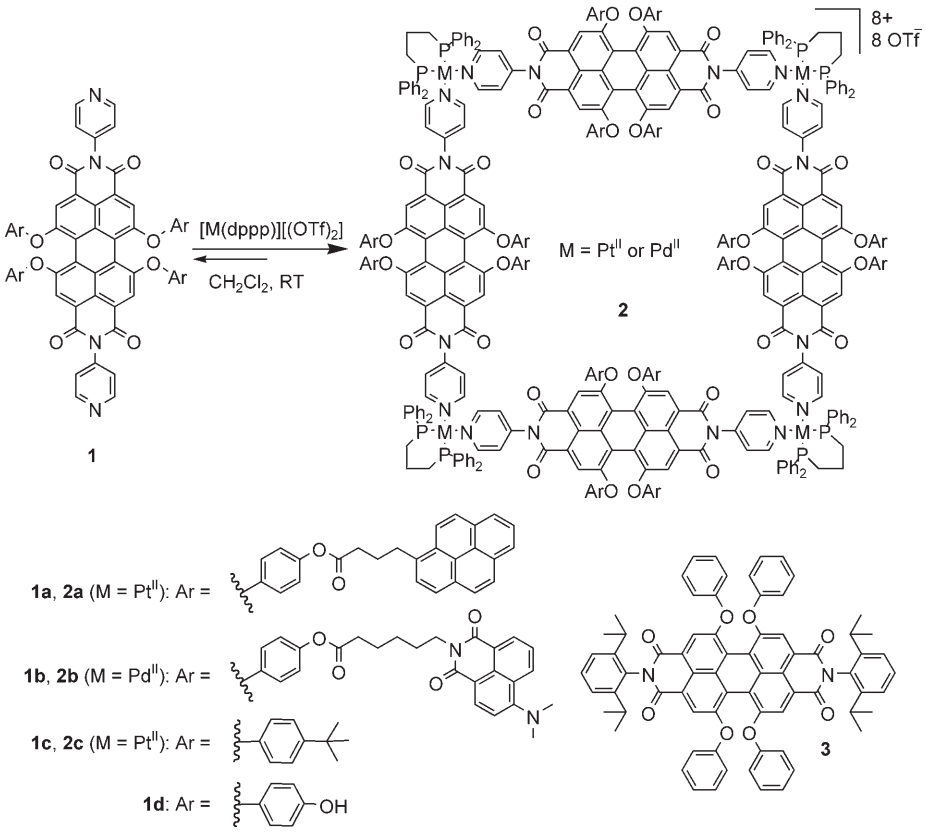

Scheme 1. Structures of pyrene- and aminonaphthalimide-functionalized and *p-tert*-butylphenyl-substituted perylene bisimide ligands **1a**,**b**,**c** and their metal-ion-mediated self-assembly into squares **2a**,**b**,**c**; perylene bisimide **1d** was used as precursor for the synthesis of ligands **1a**,**b**, and perylene bisimide **3** served as reference compound for DOSY NMR experiments (vide infra).

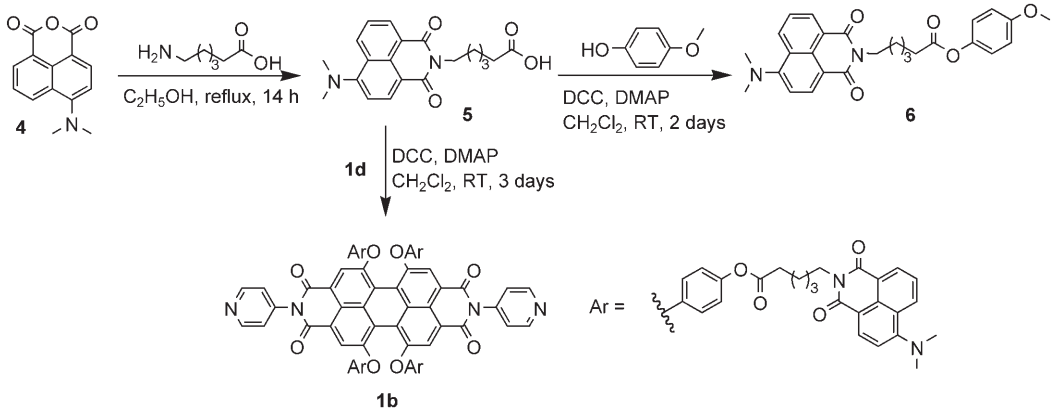

Scheme 2. Synthesis of naphthalimide-functionalized perylene bisimide ligand **1b**; DCC = dicyclohexylcarbodiimide; DMAP = 4-dimethylaminopyridine.

Results and Discussion

Synthesis of dimethylaminonaphthalimide-functionalized perylene bisimide ligand: The target ditopic perylene bisimide ligand was synthesized according to Scheme 2. For this purpose, 6-(6-dimethylamino-1,3-dioxo-1*H*,3*H*-benzo[*de*]isoquinolin-2-yl)hexanoic acid (**5**) was prepared by imidization of 4-dimethylamino-1,8-naphthalic anhydride (**4**)[11] with 6-aminohexanoic acid in dry ethanol.

Subsequently, carboxylic acid **5** was treated separately with 4-methoxyphenol and *N*,*N*′-bis(4-pyridyl)-1,6,7,12-tetrakis(4-hydroxyphenoxy)perylene-3,4:9,10-tetracarboxylic acid bisimide (**1d**)[7c] to afford reference ester **6** and the desired tetranaphthalimide-functionalized perylene bisimide ligand **1b**, respectively, through activation of the carboxyl function by dicyclohexylcarbodiimide (DCC) in the presence of 4-dimethylaminopyridine (DMAP).[7c,8] The products were purified by column chromatography (SiO_2), and ligand **1b** was obtained in pure form in 56% yield. The new compounds were fully characterized by ^1H and ^{13}C NMR spectroscopy and mass spectrometry, and correct elemental analyses were obtained (see Experimental Section).

Construction of metallosupramolecular square assembly: It is well documented that the Pd–N bond is relatively labile and its formation is reversible at ambient temperature.[6] During metal-ion-mediated self-assembly process, this property enables the conversion from initially formed linear oligomeric species to structurally well-defined macrocycles and allows the production of macrocycles in high yield.[6c] Therefore, [Pd(dppp)](OTf)$_2$ (dppp = 1,3-bis(diphenylphosphino)-propane; OTf = trifluoromethanesulfonate) was used as a 90° metal corner to make discrete macrocyclic assemblies with perylene bisimide ligand **1b**.

Initially, the metal-ion-mediated self-assembly of perylene bisimide **1b** was studied by NMR spectroscopy. Thus, an equimolar mixture of ligand **1b** and metal reagent [Pd(dppp)](OTf)$_2$ in CD_2Cl_2 exhibited a simple ^1H NMR spectrum with signal broadening and only one signal in the $^{31}P\{^1H\}$ NMR spectrum, that is, the resulting assembly has a highly symmetrical structure and its formation is quantitative. Subsequently, assembly **2b** was prepared and isolated by a conventional protocol. Ligand **1b** and metal corner [Pd(dppp)](OTf)$_2$ were mixed stoichiometrically in CH_2Cl_2 and stirred at room temperature for 24 h. After concentration, diethyl ether was added to precipitate the product, which was collected by centrifugation and dried in vacuum to afford assembly **2b** as a dark powder. Although the reaction proceeds quantitatively as monitored by NMR spectroscopy, the product could be isolated only in 79% yield due to its high solubility in CH_2Cl_2. Elemental analysis of the isolated solid fits very well with the composition of desired square assembly **2b**. To provide additional structural proof, the assembly was redissolved in CD_2Cl_2 and ^1H and $^{31}P\{^1H\}$ NMR spectra were recorded. The ^1H NMR spectrum of **2b** (Figure 1a, bottom) showed one single set of signals for the perylene ligands and the dppp moieties, and this indicates the presence of one species in solution.

The signal of the pyridyl α-protons of the ligand shifted from $\delta = 8.76$ to 9.07 ppm ($\Delta\delta = 0.31$ ppm) on assembly formation, while the upfield shift of the pyridyl β-protons by 0.15 ppm confirms metal–nitrogen coordination.[6,7] On assembly formation, the proton signals of ligands and metal corners are slightly broadened due to rotational restriction in the assembled state. The high symmetry of assembly **2b** is also supported by its $^{31}P\{^1H\}$ NMR spectrum, in which one sharp signal appears at $\delta = 7.01$ ppm, upfield-shifted by about 13 ppm compared with that of the palladium complex precursor. These spectroscopic observations are consistent with those of previously reported perylene bisimide squares,[7–9] and thus prove the square scaffold of the present assembly. The essentially identical NMR spectra that were also obtained in $CDCl_3$ confirm that the square structure is sustained in this solvent.[12]

Characterization of the square assembly by ^1H NMR diffusion-ordered spectroscopy (DOSY): The kinetic lability of Pd–N bonds facilitates the formation of structurally well-defined supramolecular assemblies but makes characterization of the corresponding supramolecular entities rather arduous.

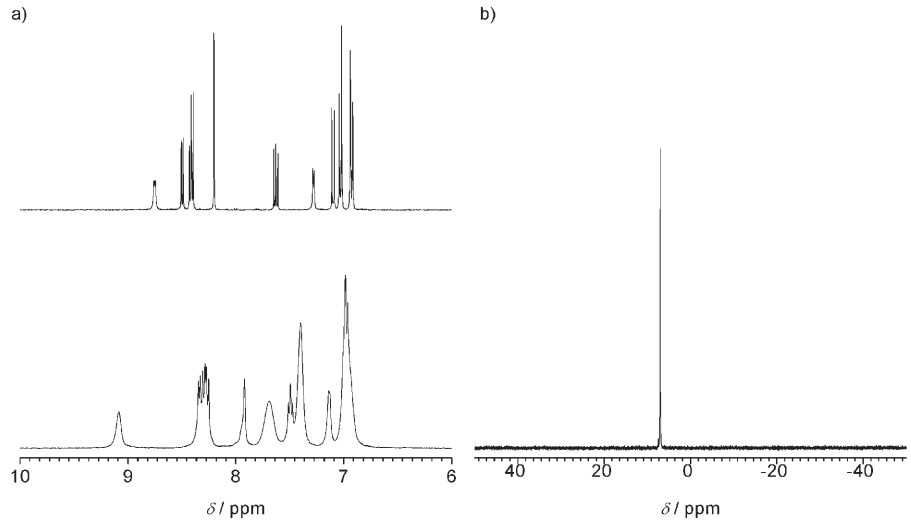

Figure 1. a) ^{1}H NMR spectra of **1b** (top) and corresponding Pd^{II} assembly **2b** (bottom) in CD_2Cl_2 (only aromatic region shown); b) $^{31}P\{^{1}H\}$ NMR spectrum of the Pd^{II} assembly **2b**.

With conventional ionization modes, satisfactory mass spectra of Pd-cornered assemblies that avoid fragmentation are not easy to obtain, although mild cold-spray ionization has recently been introduced to characterize supramolecular assemblies of this kind.[13] In this context, ^{1}H NMR DOSY[14] was performed to shed light on the diffusion properties and thus on the molecular size of assembly **2b**. The diffusion coefficient D [m^2s^{-1}] of a spherical molecule in solution can be described by the Stokes–Einstein equation $D=k_BT/6\pi\eta r_s$, that is, D is inversely proportion to the molecular dimension r_S.[15] Thus, the sizes of species can be compared based on their diffusion coefficients when the other parameters T and η are identical. Indeed, ^{1}H DOSY NMR and related techniques have recently been successfully applied to characterize a variety of metal-ion-mediated assemblies.[16]

Since the boiling point of CD_2Cl_2 (40 °C) is lower than that of $CDCl_3$ (61 °C), the DOSY experiments were performed in the latter solvent to minimize convection effects, which considerably influence the DOSY spectra with increasing diffusion time Δ in the DOSY pulse sequence. Figure 2 shows a diffusion decay curve of molecular square **2b** obtained by monitoring the ^{1}H NMR intensity at 7.94 ppm. The intensity decreases with increasing gradient strength g [$G\,cm^{-1}$] according to a Gaussian function (see Experimental Section). From the curve-fitting analysis, the diffusion coefficient was estimated as $D=5.1\times10^{-10}\,m^2s^{-1}$. Similarly, the diffusion coefficients for the same species could also be estimated from various chemical shifts. The ^{1}H DOSY NMR spectrum of square assembly **2b** (Figure 3) shows that it has a much smaller diffusion coefficient than small molecules such as water, chloroform, and TMS.

To qualitatively probe the molecular size of the square, DOSY experiments were also performed for well-characterized molecular square **2c** (Scheme 1).[7a,b] In addition, DOSY experiments were carried out to evaluate the diffusion behavior of a mixture of square **2b** and inert (without binding sites) perylene bisimide **3** (Scheme 1). Since the ^{1}H NMR spectra of these two species do not fully overlap with each other, separate evaluation of their diffusion coefficients is possible (Table 1). To make the diffusion coefficients comparable by eliminating the minor temperature and viscosity differences in each system, the D values of the investigated species were finally normalized to that of TMS as internal reference.[17]

The TMS-normalized diffusion coefficient D/D^{TMS} of square **2b** is 0.22 in $CDCl_3$. This value does not change in

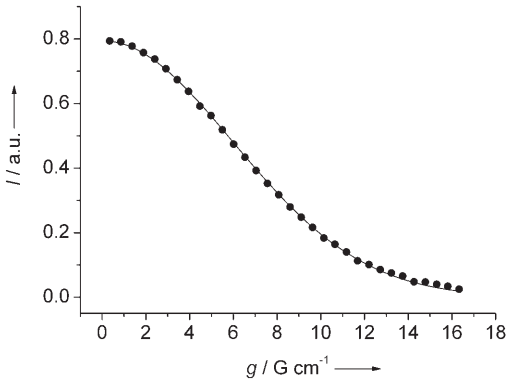

Figure 2. Observed ^{1}H NMR intensity at $\delta=7.94$ ppm of square **2b** (perylene protons) in $CDCl_3$ versus average gradient strength g [$G\,cm^{-1}$] of the sinusoidal diffusion gradients. Circles: experimental data, solid line: fitting according to Equation (4) (see Experimental Section).

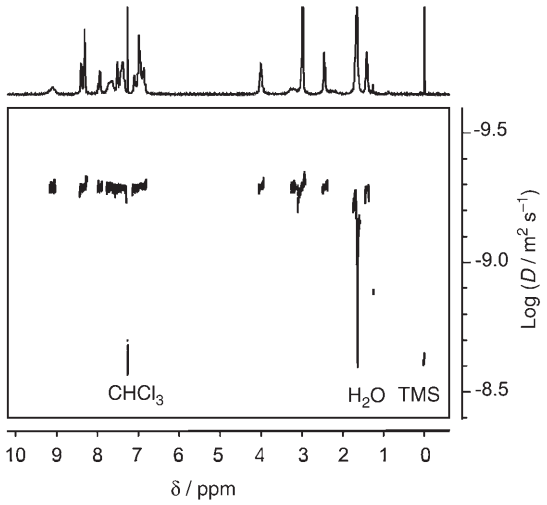

Figure 3. 600 MHz ^{1}H DOSY NMR spectrum of square assembly **2b** in $CDCl_3$ at 25 °C; 16 scans per gradient increment. The diffusion coefficients D are plotted on a logarithmic scale against the chemical shift δ.

Table 1. Diffusion coefficients of molecular squares **2b** and **2c**, perylene bisimide **3**, and TMS in $CDCl_3$ at 25 °C as obtained from ^1H DOSY NMR experiments.

Compound	D [m^2s^{-1}]	D^{TMS} [m^2s^{-1}]	D/D^{TMS}
2b	5.1×10^{-10}	23.1×10^{-10}	0.22
2b[a]	5.5×10^{-10}	24.8×10^{-10}	0.22
2c	6.1×10^{-10}	24.8×10^{-10}	0.25
3[a]	9.0×10^{-10}	24.8×10^{-10}	0.36

[a] The data were evaluated from a mixture of square **2b** and perylene bisimide **3** in $CDCl_3$.

the presence of **3**, that is, the diffusion behavior of square **2b** is not affected by compound **3**. The normalized diffusion coefficient of perylene bisimide **3** (0.36) is significantly larger than that of square **2b** (0.22). This result is just what one should expect, since the size of reference perylene bisimide **3** is comparable to that of ligand **1b**, which acts as a building block of square **2b**. This result clearly suggests that compound **3** could be used as an internal standard for the DOSY investigations of perylene bisimide assemblies. Comparison of the diffusion coefficients of the square assemblies **2b** and **2c**, which have approximately spherical geometries, reveals some interesting features. The normalized diffusion coefficient of square **2c** (0.25) is slightly larger than that of square **2b** (0.22). This finding is quite reasonable, since the additional substituents of molecular square **2b** are slightly larger than those of square **2c**. According to the Stokes–Einstein equation (vide supra), it can be estimated that the hydrodynamic radius of **2b** is about 1.14 times that of **2c**. On the basis of spherical approximation, the molecular size of **2b** is about 1.5 times that of **2c**. The latter value perfectly reflects the ratio of the molecular weights of these two assemblies (i.e., $12558/8172\approx1.5$) and thus confirms the square scaffold of the present metallosupramolecular assembly **2b** from another aspect.

Optical properties of free ligands and square assemblies: The optical properties of perylene bisimide ligand **1b** and corresponding square assembly **2b** in CH_2Cl_2 were investigated by UV/Vis and fluorescence spectroscopy. The absorption spectra of ligand **1b** and square **2b** are shown in Figure 4. Ligand **1b** shows intense absorption bands with maxima at 575 and 425 nm, which can be attributed to the perylene bisimide and dimethylaminonaphthalimide moieties, respectively. Compared with the parent chromophores, the absence of additional absorption bands indicates insignificant ground-state interaction between these two chromophores. Square **2b** exhibits a similar absorption profile, but the absorption maxima of the chromophores are shifted to 584 and 427 nm, respectively. This significant red shift (9 nm) of the perylene bisimide band further confirms coordination of the pyridyl binding sites to Lewis acidic metal ions. This bathochromic shift is still observable at the concentrations for fluorescence studies (ca. 10^{-7} M), which suggests that assembly **2b** persists even at very low concentrations. As expected, the absorption band of dimethylaminonaphthalimide moieties is barely influenced by the presence

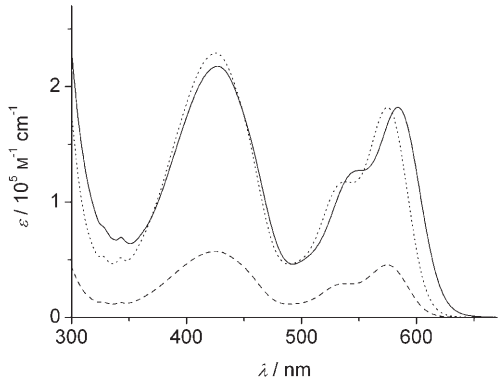

Figure 4. UV/Vis absorption spectra of free ligand **1b** (dashed line) and square **2b** (solid line) in CH_2Cl_2, and calculated UV/Vis absorption spectrum from $\varepsilon(\mathbf{1b})\times4$ (dotted line).

of Pd^{II} corners, as they are not involved in metal coordination. The similarity of the molar absorbance of assembly **2b** for both the naphthalimide and the perylene bisimide absorption bands to that of calculated spectrum for four ligands **1b** corroborates the square structure of this assembly and complies with the previous observation for perylene bisimide dye squares.[7–9]

Figure 5 shows the fluorescence spectra of ligand **1b** and square **2b** in CH_2Cl_2. Ligand **1b** exhibits an intense perylene bisimide emission at 607 nm irrespective of the excitation

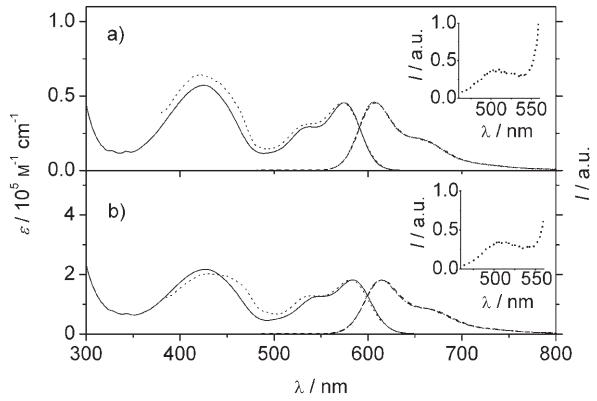

Figure 5. UV/Vis absorption (solid lines) and fluorescence emission and excitation spectra of a) ligand **1b** and b) square **2b** in CH_2Cl_2. Emission spectra were recorded by excitation at 400 (dashed lines) and 545 nm (dash-dotted lines). Excitation spectra were recorded by detection at 750 nm (dotted lines). The insets show the enlarged residual emission of dimethylaminonaphthalimide moieties.

wavelength, but also an extremely weak dimethylaminonaphthalimide emission with maximum at 500 nm on excitation at 400 nm (inset to Figure 5a). Compared with reference compound **6** (see Scheme 1), the fluorescence of aminonaphthalimide dyes in **1b** is drastically quenched (see Table 2). As excitation at 415 nm and 545 nm affords almost the same fluorescence quantum yield ($\Phi_{fl}=0.36$ and 0.38), the naphthalimide fluorescence quenching suggests a highly

Table 2. Time-resolved fluorescence data of compounds **6**, **3**, **1a**,**b**, and **2a**,**b** in CH_2Cl_2.[a]

Compound	τ [ns][b]	τ [ns]	τ [ns]
6	10.8		
3			6.0[c]
1b	0.4[d]	1.8[e]	1.9[f]
2b	0.5[g]	2.1[e]	1.9[f]
1a		0.9[h,i]	
2a		1.0[h,i]	

[a] All spectra were recorded at room temperature. [b] $\lambda_{ex}=410$ nm, $\lambda_{det}=550$ nm. [c] $\lambda_{ex}=575$ nm, $\lambda_{det}=610$ nm. [d] For compound **1b**: biexponential decay with $\tau_1=0.4$ ns (82%) and $\tau_2=2.9$ ns (18%). [e] $\lambda_{ex}=410$ nm, $\lambda_{det}=670$ nm. [f] $\lambda_{ex}=575$ nm, $\lambda_{det}=670$ nm. [g] For compound **2b**: biexponential decay with $\tau_1=0.5$ ns (93%) and $\tau_2=6.1$ ns (7%). [h] $\lambda_{ex}=324$ nm, $\lambda_{det}=615$ nm. [i] Ref. [9].

efficient energy-transfer process from peripheral dimethylaminonaphthalimide dyes to the core perylene bisimide chromophores. In the fluorescence excitation spectrum of compound **1b** ($\lambda_{det}=750$ nm) the absorption band of the antenna chromophore is observed. Therefore, the naphthalimide chromophores contribute to emission from the S_1 state of perylene bisimide and the fluorescence emission properties of multichromophore ligand **1b** are determined by the lowest energy S_1 state of the perylene bisimide unit. Square **2b** shows an emission maximum at 614 nm, which is bathochromically shifted by 7 nm relative to the free ligand (Figure 5). The fluorescence quantum yields of square **2b** were determined as $\Phi_{fl}=0.37$ and 0.41 on irradiation at 545 and 415 nm, respectively. As in the case of ligand **1b**, the fluorescence of the naphthalimide chromophores in square **2b** is also quenched, and the square assembly shows a similar profile in the fluorescence excitation spectrum.

To get more insight into the excited state properties of ligand **1b** and square **2b**, time-resolved fluorescence experiments were performed. The observed fluorescence lifetimes are compiled in Table 2, and the respective emission traces are depicted in Figure 6. On excitation of the naphthalimide units, strong quenching of their excited states was observed, as the fluorescence lifetime is drastically reduced to 0.4 and 0.5 ns for ligand **1b** and square **2b**, respectively, compared to the strongly emitting reference compound **6** ($\tau=$ 10.8 ns).[18] Nevertheless, the emission of the perylene bisimide unit is also quenched, as a lower lifetime of $\tau=1.9$ ns was observed for both ligand **1b** and square **2b** compared with that of reference perylene bisimide **3** ($\tau=6.0$). Interestingly, fluorescence quenching of perylene bisimide in **1b** and **2b** is significantly less pronounced than that observed for pyrene-containing ligand **1a** and square **2a**, as the acceptor emission decay times for the latter systems are $\tau=0.9$ and 1.0, respectively.

Based on the above-mentioned photophysical data, we assume a FRET process in light-harvesting system **2b**. Thus, the transfer rate depends on the extent of spectral overlap of the emission spectrum of the donor with the absorption spectrum of the acceptor chromophore, the quantum yield of the donor, the relative orientation of the donor and acceptor transition dipoles, and the distance between the

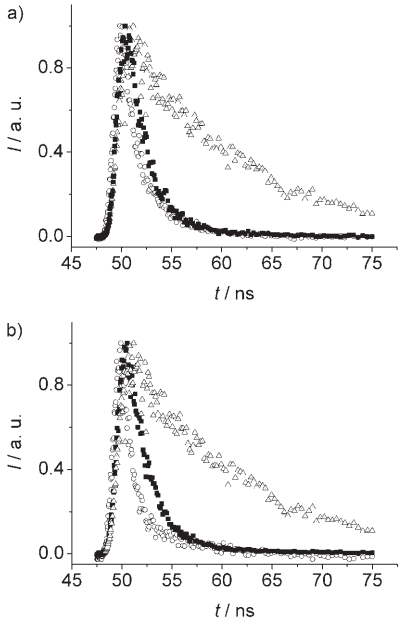

Figure 6. Time-resolved emission traces in CH_2Cl_2 with $\lambda_{ex}=410$ nm, $\lambda_{det}=550$ nm (circles) and $\lambda_{ex}=410$ nm, $\lambda_{det}=670$ nm (squares) for a) ligand **1b** and b) square **2b**. In both diagrams the emission trace of naphthalimide reference compound **6** is shown for comparison (triangles).

donor and acceptor molecules.[19] The Förster distance R_0 (distance at which energy-transfer efficiency is 50%) is typically in the range of 20–60 Å and can be calculated according to Equation (1), where κ^2 is the orientation factor, n the refractive index of the medium, Φ_D the fluorescence quantum yield of the donor in the absence of acceptor, and $J(\lambda)$ the overlap integral of the donor emission and acceptor absorption spectra. By employing Equation (1), R_0 is calculated for compound **2b** as 48.5 Å, with $\kappa^2=2/3$, $n(CH_2Cl_2)=1.4240$, $\Phi_D(CH_2Cl_2)=0.49$ (determined relative to quinine sulfate in 1.0 N H_2SO_4, $\Phi_{fl}=0.55$[20a]) and $J(\lambda)=1.87\times10^{15}\,M^{-1}cm^{-1}nm^4$ (calculated from the optical spectra of reference compounds **6** and **3**). The rate of energy transfer from a donor to an acceptor is given by Equation (2).

$$R_0 = 0.211\,[\kappa^2 n^{-4}\Phi_D J(\lambda)]^{1/6} \quad (1)$$

$$k_T(r) = 1/\tau_{DA} - 1/\tau_D = (1/\tau_D)(R_0/r)^6 \quad (2)$$

With a τ_{DA} value of 0.5 ns (decay of the donor in the presence of acceptor) and a τ_D value of 10.8 ns (decay of the donor in the absence of acceptor), k_T is calculated as $1.91\times10^9\,s^{-1}$ for square assembly **2b** (for lifetime data, see Table 2). Thus, the efficiency of the energy transfer can be calculated as $E=0.95$ according to Equation (3).

$$E = 1-(\tau_{DA}/\tau_D) \quad (3)$$

Given the values for R_0 and k_T, the donor–acceptor distance can be calculated as $r=29.3$ Å by employing Equa-

tion (2). This value is about 33% higher than the interchromophore distance of 22 Å derived from molecular modeling studies (which results in an estimated value of $k_T = 1.06 \times 10^{10}\ s^{-1}$). On the other hand, the energy-transfer efficiency can also be calculated on the basis of the integration of the fluorescence emission curve of naphthalimide before and after attachment to the perylene bisimide.[19c] Accordingly, a value of $E = 0.99$ is determined that leads to an estimation of $\tau_{DA} = 108$ ps, $k_T = 9.17 \times 10^9\ s^{-1}$, and $r = 22.5$ Å. The discrepancy between these values derived from time-resolved and steady-state fluorescence spectroscopy can be attributed to the following reasons: First, the value of R_0 according to Equation (1) is poorly assessed because of the simplified assumption of the dipole–dipole orientation factor $\kappa^2 = 2/3$, which is strictly valid only for a random orientation of the chromophores.[19] In the present case, however, the naphthalimide donor and the perylene bisimide acceptor are covalently bound and their orientation is sterically constrained. Therefore, this assumption introduces an error into the calculation of the energy-transfer efficiency. Second, the time resolution of our fluorescence experimental setup is about 300 ps; rate constants of faster processes cannot be resolved adequately. This results in a pronounced error in τ_{DA} and, consequently, in the r value. Taking these factors into account, it is reasonable to set 95% as the lower limit of the energy transfer efficiency of this naphthalimide–perylene bisimide conjugate.

The fluorescence quantum yields Φ_{fl} for ligand **1b** in various solvents and for square **2b** in CH_2Cl_2 were determined relative to *N*,*N*′-bis(2,6-diisopropylphenyl)-1,6,7,12-tetraphenoxyperylene-3,4:9,10-tetracarboxylic acid diimide ($\Phi_{fl} = 0.96$ in $CHCl_3$)[20a] by using the optical-dilution method.[20b,21] The Φ_{fl} data of the present naphthalimide-containing ligand **1b** and square **2b** and, for comparison, those of previously reported[9] pyrene-functionalized systems **1a** and **2a** are given in Table 3.

Table 3. Fluorescence emission properties of ligands **1a**,**b** and squares **2a**,**b**.

Compound	Solvent	Relative permittivity ε_r	λ_{em} [nm]	Φ_{fl}
1b	dioxane	2.21	596	0.37
	THF	7.58	595	0.22
	CH_2Cl_2	8.93	607	0.38[a]
2b	CH_2Cl_2	8.93	614	0.37[b]
1a	CH_2Cl_2	8.93	611	0.12[c,e]
2a	CH_2Cl_2	8.93	619	0.05[d,e]

[a] $\lambda_{ex} = 545$ nm (on excitation at 415 nm a quantum yield of $\Phi_{fl} = 0.36$ was observed).[b] $\lambda_{ex} = 545$ nm (on excitation at 415 nm a quantum yield of $\Phi_{fl} = 0.41$ was observed).[c] $\lambda_{ex} = 336$ and 545 nm. [d] $\lambda_{ex} = 307$ and 550 nm. [e] Ref. [9].

No general trend for the effect of solvent polarity on fluorescence quantum yield of ligand **1b** could be observed, as Φ_{fl} values of 0.36 in CH_2Cl_2 ($\varepsilon_r = 8.93$), 0.37 in dioxane ($\varepsilon_r = 2.21$), and 0.22 in THF ($\varepsilon_r = 7.58$) were determined. It was reported that the fluorescence quantum yield of *N*,*N*′-bis(4-pyridyl)-1,6,7,12-tetra(4-hexanoyloxyphenoxy)perylene-3,4:9,10-tetracarboxylic acid bisimide, which can be taken as a model compound for perylene bisimide ligands **1a**,**b**, is 0.90 in CH_2Cl_2.[22] In comparison to this model system, the luminescence of the perylene bisimide moiety in pyrene-containing ligand **1a** ($\Phi_{fl} = 0.12$)[9] is decreased by about 87%, and in respective square **2a** ($\Phi_{fl} = 0.05$)[9] it is even more strongly diminished, while for the present aminonaphthalimide-functionalized systems **1b** ($\Phi_{fl} = 0.36$) and **2b** ($\Phi_{fl} = 0.37$) significantly less pronounced fluorescence quenching was observed. As the $S_1 \rightarrow S_0$ transition energy of the perylene bisimide units (ca. 2.04 eV) is higher than the energy level of the charge-separated state in polar solvents ($Perlyene^{\bullet-}$-$Naph^{\bullet+}$, ca. 1.75 eV)[7,23] by about 0.3 eV, a photoinduced intramolecular electron-transfer process is thermodynamically feasible and seems to account for such fluorescence quenching. Nevertheless, the square scaffold **2b** with naphthalimide antenna chromophores has a more than seven times greater fluorescence ability than pyrene-containing square **2a**. Owing to their significant absorbance of blue light (see spectra in Figure 4), these novel squares are indeed efficient light-harvesting multichromophore assemblies.

Conclusion

Fluorescent dimethylaminonaphthalimide dyes were attached at the bay area of a bis-pyridyl perylene bisimide chromophore, and self-assembly of this ditopic ligand, directed by metal-ion coordination, afforded a fluorescent multichromophore square scaffold incorporating sixteen aminonaphthalimide antenna dyes and four central perylene bisimide dyes. Steady-state and time-resolved fluorescence investigations showed that the blue-light energy absorbed by the peripheral dimethylaminonaphthalimide units can be efficiently transferred to the core perylene bisimide dyes through a fluorescent resonance energy transfer (FRET) mechanism. Bright emission with more than seven times higher fluorescence quantum yield was observed for the aminonaphthalimide-containing square assembly **2b** compared with that of the previously reported pyrene-functionalized system **2a**.

Experimental Section

Materials: Solvents and reagents were obtained from commercial suppliers, unless otherwise stated, and purified and dried according to standard procedures.[24] 4-Dimethylamino-1,8-naphthalic anhydride (**4**),[11] *N*,*N*′-bis(4-pyridyl)-1,6,7,12-tetra(4-hydroxylphenoxy)perylene-3,4:9,10-tetracarboxylic acid bisimide (**1d**),[7c] and [Pt(dppp)](OTf)$_2$·2H$_2$O (dppp = 1,3-bis(diphenylphosphino)propane, OTf = trifluoromethanesulfonate),[25] molecular square **2c**,[7a,b] and *N*,*N*′-bis(2,6-diisopropylphenyl)-1,6,7,12-tetraphenoxyperlyene-3,4:9,10-tetracarboxylic acid bisimide (**3**)[26] were prepared according to literature procedures. Column chromatography was performed on silica gel (Merck Silica 60, particle size 0.04–0.063 mm). The solvents for spectroscopic studies were of spectroscopic grade and used as received.

6-(6-Dimethylamino-1,3-dioxo-1*H*,3*H*-benzo[*de*]isoquinolin-2-yl)hexanoic acid (5): 4-Dimethylamino-1,8-naphthalic anhydride (**4**; 2.42 g, 10.0 mmol) and 6-aminohexanoic acid (5.25 g, 40.0 mmol) were suspended in dry ethanol (100 mL). The reaction mixture was heated to reflux and stirred for 14 h. After cooling to room temperature, unconsumed 6-aminohexanic acid was removed by filtration and the filtrate was evaporated to dryness. The residue was dissolved in CH_2Cl_2, which was washed successively with dilute hydrochloric acid (1 M) and water. After drying over Na_2SO_4 and filtration, dichloromethane was evaporated under reduced pressure. The obtained residue was subjected to column chromatography (SiO_2) with CH_2Cl_2/EtOH (95/5) as eluent. The desired fractions were collected and evaporated to afford a yellow solid. Yield: 1.45 g (41 %); m.p. 139–140 °C; ^{1}H NMR (400 MHz, $CDCl_3$, TMS): $\delta =$ 8.56 (d, 1H, H_{ar}), 8.47 (d, ^3J(H,H) = 8.3 Hz, 1H, H_{ar}), 8.43 (d, 1H, H_{ar}), 7.65 (dd, 1H, H_{ar}), 7.11 (d, ^3J(H,H) = 8.3 Hz, 1H, H_{ar}), 4.17 (t, 2H, CH_2), 3.10 (s, 6H, CH_3), 2.37 (t, 2H, CH_2), 1.74 (m, 4H, CH_2), 1.48 (m, 2H, CH_2); ^{13}C NMR (100 MHz, $CDCl_3$, TMS): $\delta =$ 179.16, 164.60, 164.08, 155.77, 132.65, 131.12, 131.07, 130.22, 125.28, 124.96, 123.08, 115.16, 113.42, 44.82, 39.94, 33.87, 27.76, 26.57, 24.42; MS (70 eV, EI): *m*/*z*: 354.1 $[M]^+$; elemental analysis calcd (%) for $C_{20}H_{22}N_2O_4$ (354.41): C 67.78, H 6.26, N 7.90; found: C 67.60, H 6.29, N 7.70.

6-(6-Dimethylamino-1,3-dioxo-1*H*,3*H*-benzo[*de*]isoquinolin-2-yl)hexanoic acid 4-methoxyphenyl ester (6): A mixture of 4-methoxyphenol (124 mg, 1.0 mmol), 6-(6-dimethylamino-1,3-dioxo-1*H*,3*H*-benzo[*de*]isoquinolin-2-yl)hexanoic acid **5** (355 mg, 1.0 mmol), DMAP (100 mg), and DCC (300 mg) in dry CH_2Cl_2 (30 mL) was stirred at room temperature for 48 h. The undissolved materials were removed by filtration and the filtrate was evaporated on a rotavapor to dryness. The residue was purified by column chromatography (SiO_2) with CH_2Cl_2/CH_3OH (98/2) as eluent. The desired fractions were collected and evaporated to afford a bright yellow solid. Yield: 310 mg (67 %); m.p. 75–77 °C; ^{1}H NMR (400 MHz, $CDCl_3$, TMS): $\delta =$ 8.57 (d, 1H, H_{ar}), 8.48 (d, ^3J(H,H) = 8.3 Hz, 1H, H_{ar}), 8.44 (d, 1H, H_{ar}), 7.66 (dd, 1H, H_{ar}), 7.12 (d, ^3J(H,H) = 8.3 Hz, 1H, H_{ar}), 6.97 (d, ^3J(H,H) = 9.1 Hz, 2H, H_{ar}), 6.85 (d, ^3J(H,H) = 9.1 Hz, 2H, H_{ar}), 4.20 (t, 2H, CH_2), 3.78 (s, 3H, -CH_3), 3.10 (s, 6H, CH_3), 2.55 (t, 2H, CH_2), 1.82 (m, 4H, CH_2), 1.55 (m, 2H, CH_2); ^{13}C NMR (100 MHz, $CDCl_3$, TMS): $\delta =$ 172.49, 164.63, 164.10, 157.14, 156.91, 144.29, 132.64, 131.14, 131.04, 130.27, 125.37, 124.94, 123.15, 122.34, 115.16, 114.41, 113.40, 55.58, 44.81, 39.95, 34.23, 27.81, 26.63, 24.74; UV/Vis (CH_2Cl_2): λ_{max} (ε) = 416 nm (11 150 $M^{-1}cm^{-1}$); MS (70 eV, EI): *m*/*z*: 460.1 $[M]^+$; elemental analysis (%) calcd for $C_{27}H_{28}N_2O_5$ (460.53): C 70.42, H 6.13, N 6.08; found: C 70.32, H 6.36, N 6.09.

***N,N′*-Bis(4-pyridyl)-1,6,7,12-tetrakis{4-[6-(6-dimethylamino-1,3-dioxo-1*H*,3*H*-benzo[*de*]isoquinolin-2-yl]hexanoyloxyphenoxy}perylene-3,4:9,10-tetracarboxylic acid bisimide (1b)**: Perylene bisimide **1d** (109 mg, 0.1 mmol), hexanoic acid **5** (213 mg, 0.6 mmol), DCC (500 mg), and DMAP (200 mg) were suspended in dry CH_2Cl_2 (25 mL) and stirred at room temperature for three days. The undissolved materials were removed by filtration and the filtrate was evaporated to dryness. The residue was purified by column chromatography (SiO_2) with CH_2Cl_2/THF (80/20) as eluent. The desired fractions were collected and concentrated on a rotavapor. Subsequently, *n*-hexane was added to precipitate the product, which was collected by centrifugation. Yield: 130 mg (56 %); m.p. 261–263 °C; ^{1}H NMR (400 MHz, $CDCl_3$, TMS): $\delta =$ 8.79 (d, 4H, $H_{\alpha\text{-py}}$), 8.55 (d, 4H, H_{ar}), 8.46 (d, 4H, H_{ar}), 8.41 (d, 4H, H_{ar}), 8.24 (s, 4H, H_{per}), 7.64 (dd, 4H, H_{ar}), 7.42 (d, 4H, $H_{\beta\text{-py}}$), 7.11 (d, 4H, H_{ar}), 7.03 (d, 8H, H_{ar}), 6.90 (d, 8H, H_{ar}), 4.18 (t, 8H, CH_2), 3.09 (s, 24H, CH_3), 2.56 (t, 8H, CH_2), 1.81 (m, 16H, CH_2), 1.54 (m, 8H, CH_2); ^{13}C NMR (100 MHz, $CDCl_3$, TMS): $\delta =$ 171.83, 164.60, 164.05, 162.22, 156.93, 155.82, 152.44, 147.46, 132.92, 132.63, 131.13, 131.01, 130.24, 125.32, 124.91, 123.35, 123.11, 122.50, 121.08, 121.01, 120.18, 120.07, 115.07, 113.37, 44.79, 39.90, 34.20, 27.76, 26.59, 24.61; UV/Vis (CH_2Cl_2): λ_{max} (ε) = 575 (45 500), 537 (29 400), 425 nm (57 200 $M^{-1}cm^{-1}$); MS (MALDI-TOF, dithranol): *m*/*z*: 2323.1 $[M+H]^+$; elemental analysis (%) calcd for $C_{138}H_{112}N_{12}O_{24}$ (2322.47): C 71.37, H 4.86, N 7.24; found C 70.87, H 5.17, N 7.08.

Perylene bisimide-walled palladium-cornered square 2b: An equimolar mixture of perylene bisimide ligand **1b** (23.2 mg, 10.0 μmol) and [Pd(dppp)](OTf)$_2$·2H$_2$O (8.53 mg, 10.0 μmol) in dry CH_2Cl_2 (5 mL) was stirred at room temperature for 24 h. After filtration, the solution was concentrated to about 1 mL, and diethyl ether (10 mL) was added to precipitate the product, which was collected by centrifugation. After the product was dried in vacuum, a dark powder was obtained. Yield: 25 mg (79 %); m.p. 227–230 °C; ^{1}H NMR (400 MHz, CD_2Cl_2, $\delta =$ 5.32 ppm): $\delta =$ 9.07 (br s, 16H, $H_{\alpha\text{-py}}$), 8.30 (m, 48H, H_{ar}), 7.92 (s, 16H, H_{per}), 7.68 (br s, 32H, $H_{ar(dppp)}$), 7.50 (t, 16H, H_{ar}), 7.40 (br s, 48H, $H_{ar(dppp)}$), 7.13 (d, ^3J(H,H) = 5.1 Hz, 16H, $H_{\beta\text{-py}}$), 6.99 (m, 80H, H_{ar}), 3.93 (br, 32H, CH_2), 3.24 (br s, 16H, $H_{CH2(dppp)}$), 2.97 (s, 96H, CH_3), 2.44 (br, 32H, CH_2), 2.29 (br s, 8H, $H_{CH2(dppp)}$), 1.64 (m, 64H, CH_2), 1.38 (m, 32H, CH_2); ^{13}C NMR (100 MHz, CD_2Cl_2, $\delta =$ 54.0 ppm): $\delta =$ 172.31, 164.65, 164.09, 161.89, 157.32, 156.29, 153.19, 151.65, 148.01, 146.00, 133.54, 133.24, 133.08, 132.72, 131.40, 130.98, 130.53, 130.37, 127.54, 125.58, 125.26, 123.79, 123.50, 123.34, 122.46, 121.43, 121.03, 120.15, 120.03, 115.28, 113.72, 45.07, 40.10, 34.54, 28.22, 26.99, 25.04, 22.02, 18.18; ^{31}P{^{1}H} NMR (162 MHz, CD_2Cl_2, 85 % H_3PO_4): $\delta =$ 7.01 (s); UV/Vis (CH_2Cl_2): λ_{max} (ε) = 584 (182 000), 550 (127 000), 427 nm (218 000 $M^{-1}cm^{-1}$); elemental analysis (%) calcd for $C_{668}H_{552}F_{24}N_{48}O_{120}P_8Pd_4S_8$·8H$_2$O (12 702.01): C 63.17, H 4.51, N 5.29, S 2.02; found: C 63.05, H 4.46, N 5.41, S 1.90.

Spectroscopic measurements: ^{1}H and ^{13}C NMR spectra were recorded on a Bruker Avance 400 spectrometer with TMS or residual undeuterated solvent as internal standard. The ^{31}P{^{1}H} NMR spectra were recorded at 162 MHz, and chemical shifts are reported relative to external 85 % aqueous H_3PO_4 ($\delta = 0$ ppm). MALDI-TOF spectra were recorded on a Bruker Franzen Reflex III spectrometer. UV/Vis spectra were measured in a conventional quartz cell (light path 10 mm) on a Perkin-Elmer Lambda 40P spectrophotometer at room temperature (ca. 20 °C).

^{1}H DOSY NMR spectroscopy: ^{1}H DOSY[14] experiments were carried out at 25 °C on a Bruker DMX 600 spectrometer equipped with a BGPA 10 gradient generator, a BGU II control unit, and a conventional 5-mm broadband (^{15}N-^{31}P)/^{1}H probe with automatic tune/match accessory and *z* axis gradient coil. Data were acquired and processed using the Bruker software XWIN-NMR 3.5, patch level 6. The longitudinal eddy current delay sequence with bipolar gradient pulse pairs for diffusion (BPP-LED)[26] and additional sinusoidal spoil gradients after the second and forth 90° pulses was used with the following acquisition parameters: duration δ of a bipolar gradient pulse: 4.4 ms (2 × 2.2 ms), diffusion time Δ: 200 ms, spoiler gradient duration: 1.1 ms, spoiler gradient strengths: 2.9 and 2.3 G cm^{-1} average (4.7 and 3.6 G cm^{-1} peak), eddy current delay: 5 ms, delay τ between the gradients of a bipolar gradient pulse pair: 0.3 ms. The sinusoidal diffusion gradients were incremented from 0.3 to 16.3 G cm^{-1} average gradient strength (corresponding to 0.5 to 25.9 G cm^{-1} peak gradient strength) in 32 linear steps with 16–128 scans per step for signal averaging. The ^{1}H NMR data were recorded in $CDCl_3$ solutions in 5 mm NMR tubes and referenced to internal TMS.

The strength of the pulsed magnetic field gradients was calibrated by a ^{1}H DOSY experiment on a sample of 1 % H_2O in 99 % D_2O, doped with 0.1 mg mL^{-1} $GdCl_3$ to achieve short spin–lattice relaxation times, by using the known value of the diffusion coefficient for H_2O at 25 °C in this H_2O/D_2O mixture.[28] For this calibration experiment a diffusion time Δ of 50 ms and identical pulsed field gradient parameters were used as for the perylene bisimide compounds.

The DOSY spectra were calculated using the Bruker software XWIN-NMR 3.5, patch level 6. For this purpose, a Levenberg–Marquardt algorithm was used for one-component fittings of the dependence of the signal intensities to gradient strength according to Equation (4) for each data point in the ^{1}H spectrum with D and I_0 as adjustable parameters. The widths of the peaks in the diffusion dimension correlate with the fitting error. In addition, fittings for the individual ^{1}H signals according to Equation (4) were performed to judge the quality of the DOSY spectrum.

$$I = I_0 \exp[-D\gamma^2 g^2 \delta^2 (\Delta - \delta/3 - \tau/2)] \quad (4)$$

The diffusion coefficient D in Equation (4) represents the result of the fitting procedure, I_0 is the fitted signal intensity for zero gradient strength, I the observed intensity for the average gradient strength g, γ

the gyromagnetic ratio of the observed nuclei, and τ the delay between the two pulses of a bipolar gradient pulse pair.

A relatively long diffusion time Δ of 200 ms had to be used due to hardware limitations of the gradient unit and the relatively small diffusion coefficients of the molecules under investigation. Therefore, the DOSY results are expected to be influenced by convection effects which are introduced by unavoidable temperature gradients in the sample and become increasingly more pronounced with increasing diffusion time. Qualitatively, however, the differences in diffusion properties of the different species under investigation proved to be sufficient to draw plausible conclusions. In particular, since convection effects are expected to increase the measured diffusion coefficients of all species present in the sample by the same absolute amount, the relative increase of the measured D values is more pronounced for large molecules which diffuse slowly than for faster diffusing smaller species. Therefore, the differences between the measured diffusion coefficients for the molecules of different sizes should be even larger in the absence of convection effects.

Optical spectra: Fluorescence emission and excitation spectra were recorded in a conventional rectangular quartz cell ($10\times10\times40$ mm) on a PTI QM4-2003 fluorescence spectrometer and are corrected against photomultiplier and lamp intensity. A long wavelength range emission-corrected photomultiplier R928 was used. Fluorescence quantum yields were determined under dilute conditions ($A<0.05$) in CH_2Cl_2 versus *N,N′*-(2,6-diisopropylphenyl)-1,6,7,12-tetraphenoxyperylene-3,4:9,10-tetracarboxylic acid bisimide ($\Phi_{fl}=0.96$ in $CHCl_3$) as reference.[20,21] Fluorescence lifetimes were measured with a PTI Laser Strobe fluorescence lifetime spectrometer system containing a PTI GL-3300 nitrogen laser (337.1 nm, pulse width 600 ps, pulse energy 1.45 mJ) coupled with a dye laser PTI GL302 (pulse width 500 ps, pulse energy 220 μJ at 550 nm) as an excitation source and stroboscopic detection. Laser output was tuned within the emission curves of the laser dyes supplied by the manufacturer (PLD 421, 500, 579, 665, 735). Details of the Laser Strobe systems are described on the manufacturer's web site[29] and in the literature.[30] The instrument response function was collected by scattering the exciting light of a dilute, aqueous suspension of silica (LUDOX). Decay curves were evaluated by using the software supplied with the instrument with application of least-squares regression analysis. The quality of the fit was evaluated by analysis of χ^2, *DW* factor, and *Z* value as well as by inspection of residuals and autocorrelation function. The experiments were performed at room temperature. No attempt was made to remove O_2 from the samples.

Acknowledgements

We thank the Alexander von Humboldt Foundation (postdoctoral fellowship for C.C.Y.), the Fonds der Chemischen Industrie (Kekulé doctoral fellowship for C.H.), and the Volkswagen Foundation for financial support. The BASF AG and umicore AG are acknowledged for the donation of chemicals.

[1] a) T. Pullerits, V. Sundström, *Acc. Chem. Res.* **1996**, *29*, 381–389; b) T. Ritz, A. Damjanović, K. Schulten, *ChemPhysChem* **2002**, *3*, 243–248; c) X. Hu, T. Ritz, A. Damjanović, F. Autenrieth, K. Schulten, *Q. Rev. Biophys.* **2002**, *35*, 1–62.

[2] a) G. McDermott, S. M. Prince, A. A. Freer, A. M. Hawthornthwaite-Lawless, M. Z. Papiz, R. J. Cogdell, N. W. Isaacs, *Nature* **1995**, *374*, 517–521; b) A. W. Roszak, T. D. Howard, J. Southall, A. T. Gardiner, C. J. Law, N. W. Isaacs, R. J. Cogdell, *Science* **2003**, *302*, 1969–1972.

[3] For a recent compilation of multichromophore dye assemblies, see *Supramolecular Dye Chemistry, Topics in Current Chemistry, Vol. 258* (Ed.: F. Würthner), Springer, Berlin, **2005**.

[4] For reviews on light-harvesting dendrimers, see a) V. Balzani, S. Campagna, G. Denti, A. Juris, S. Serroni, M. Venturi, *Acc. Chem. Res.* **1998**, *31*, 26–34; b) G. R. Newkome, E. He, C. N. Moorefield, *Chem. Rev.* **1999**, *99*, 1689–1746; c) *Dendrimers and Other Dendritic Polymers* (Eds.: J. M. J. Frechét, D. A. Tomalia), Wiley, New York, **2002**; d) A. Dirksen, L. C. R. De Cola, *Chimia* **2003**, *57*, 873–882; e) F. C. De Schryver, T. Vosch, M. Cotlet, M. van der Auweraer, K. Müllen, J. Hofkens, *Acc. Chem. Res.* **2005**, *38*, 514–522.

[5] Recent reviews: a) A. Satake, Y. Kobuke, *Tetrahedron* **2005**, *61*, 13–41; b) C.-C. You, R. Dobrawa, C. R. Saha-Möller, F. Würthner, *Top. Curr. Chem.* **2005**, *258*, 39–82.

[6] For recent reviews, see: a) M. Fujita, *Chem. Soc. Rev.* **1998**, *27*, 417–425; b) S. Leininger, B. Olenyuk, P. J. Stang, *Chem. Rev.* **2000**, *100*, 853–908; c) B. J. Holliday, C. A. Mirkin, *Angew. Chem.* **2001**, *113*, 2076–2097; *Angew. Chem. Int. Ed.* **2001**, *40*, 2022–2043; d) F. Würthner, C.-C. You, C. R. Saha-Möller, *Chem. Soc. Rev.* **2004**, *33*, 133–146; e) M. Schmittel, V. Kalsani, *Top. Curr. Chem.* **2005**, *245*, 1–53; f) C. H. M. Arrijs, G. P. M. van Klink, G. van Koten, *Dalton Trans.* **2006**, 308–327.

[7] a) F. Würthner, A. Sautter, *Chem. Commun.* **2000**, 445–446; b) F. Würthner, A. Sautter, D. Schmid, P. J. A. Weber, *Chem. Eur. J.* **2001**, *7*, 894–902; c) C.-C. You, F. Würthner, *J. Am. Chem. Soc.* **2003**, *125*, 9716–9725.

[8] F. Würthner, A. Sautter, *Org. Biomol. Chem.* **2003**, *1*, 240–243.

[9] A. Sautter, B. K. Kaletas, D. G. Schmid, R. Dobrawa, M. Zimine, G. Jung, I. H. M. van Stokkum, L. De Cola, R. M. Williams, F. Würthner, *J. Am. Chem. Soc.* **2005**, *127*, 6719–6729.

[10] a) S. Saha, A. Samanta, *J. Phys. Chem. A* **2002**, *106*, 4763–4771; b) T. Philipova, *J. Prakt. Chem.* **1994**, *336*, 587–590.

[11] a) H. G. Rule, S. B. Thompson, *J. Chem. Soc.* **1937**, 1764–1767; b) V. L. Plakidin, V. N. Vostrova, *Russ. J. Org. Chem.* **1981**, *17*, 990–991.

[12] In the fabrication of metallosupramolecular square assemblies in $CDCl_3$, special attention must be paid to the quality of the solvent used. Photopromoted oxidation of $CDCl_3$ usually leads to the presence of minor amount of hydrochloric acid in the solvent, which might spoil the square assemblies by blocking the pyridyl binding sites.

[13] For mass spectrometric characterization of metallosupramolecular assemblies, see: a) C. A. Schalley, *Mass Spectrom. Rev.* **2001**, *20*, 253–309; b) S. Sakamoto, M. Fujita, K. Kim, K. Yamaguchi, *Tetrahedron* **2000**, *56*, 955–964.

[14] For comprehensive reviews on DOSY NMR, see: a) C. S. Johnson Jr., *Prog. Nucl. Magn. Reson. Spectrosc.* **1999**, *34*, 203–256; b) Y. Cohen, L. Avram, L. Frish, *Angew. Chem.* **2005**, *117*, 524–560; *Angew. Chem. Int. Ed.* **2005**, *44*, 520–554.

[15] a) H. J. V. Tyrrell, K. R. Harris, *Diffusion in Liquids: A Theoretical and Experimental Study*, Butterworths, London, **1984**; b) E. L. Cussler, *Diffusion: Mass Transfer in Fluid Systems*, Cambridge University Press, Cambridge, **1984**.

[16] a) U. Michelsen, C. A. Hunter, *Angew. Chem.* **2000**, *112*, 780–783; *Angew. Chem. Int. Ed.* **2000**, *39*, 764–767; b) A. Hori, K. Kumazawa, T. Kusukawa, D. K. Chand, M. Fujita, S. Sakamoto, K. Yamaguchi, *Chem. Eur. J.* **2001**, *7*, 4142–4149; c) R. Dobrawa, M. Lysetska, P. Ballester, M. Grüne, F. Würthner, *Macromolecules* **2005**, *38*, 1315–1325; d) T. Megyes, H. Jude, T. Grosz, I. Bako, T. Radnai, G. Tarkanyi, G. Palinkas, P. J. Stang, *J. Am. Chem. Soc.* **2005**, *127*, 10731–10738.

[17] E. J. Cabrita, S. Berger, *Magn. Reson. Chem.* **2001**, *39*, S142–S148.

[18] In both cases a biexponential decay with a minor component of a long-lived species was observed. Owing to concomitant excitation of both naphthalimide and perylene bisimide chromophores at 550 nm, this minor component can be attributed to the fluorescence of the simultaneously emitting perylene bisimide chromophore.

[19] a) T. Förster, *Ann. Phys.* **1948**, 55–75; b) J. R. Lakowicz, *Principles of Fluorescence Spectroscopy*, Kluwer Academic/Plenum Publishers, New York, **1999**, pp. 367–394; c) B. Valeur, *Molecular Fluorescence: Principles and Applications*, VCH, Weinheim, **2001**, pp. 247–272.

[20] a) R. Gvishi, R. Reisfeld, Z. Burshtein, *Chem. Phys. Lett.* **1993**, *213*, 338–344; b) J. N. Demas, G. A. Crosby, *J. Phys. Chem.* **1971**, *75*, 991–1024.

[21] A. Credi, L. Prodi, *Spectrochim. Acta, Spectrochim. Acta Part A* **1998**, *54*, 159–170.

[22] B. K. Kaletas, R. Dobrawa, A. Sautter, F. Würthner, M. Zimine, L. De Cola, R. M. Williams, *J. Phys. Chem. A* **2004**, *108*, 1900–1909.
[23] S. R. Greenfield, W. A. Svec, D. Gosztola, M. R. Wasielewski, *J. Am. Chem. Soc.* **1996**, *118*, 6767–6777.
[24] D. D. Perrin, W. L. F. Armarego, *Purification of Laboratory Chemicals*, 2nd ed., Pergamon Press, Oxford, **1980**.
[25] P. J. Stang, D. H. Cao, S. Saito, A. M. Arif, *J. Am. Chem. Soc.* **1995**, *117*, 6273–6283.
[26] G. Seybold, G. Wagenblast, *Dyes Pigm.* **1989**, *11*, 303–317.
[27] D. Wu, A. Chen, C. S. Johnson, Jr., *J. Magn. Reson. A* **1995**, *115*, 260–264.
[28] M. Holz, H. Weingärtner, *J. Magn. Reson.* **1991**, *92*, 115–125.
[29] http://www.pti-nj.com.
[30] R. G. Bennett, *Rev. Sci. Instrum.* **1960**, *31*, 1275–1279.

Received: March 24, 2006
Published online: July 25, 2006

